J. Biochem. 132, 713–718 (2002)

Role of a Conserved J8/7 X P4 Base-Triple in the *Tetrahymena* Ribozyme[1]

Yasushi Ohki, Yoshiya Ikawa, Hideaki Shiraishi, and Tan Inoue[2]

Graduate School of Biostudies, Kyoto University, Kyoto 606-8502

Received June 17, 2002; accepted August 10, 2002

The *Tetrahymena* group I intron ribozyme folds into a complex three dimensional structure for performing the self-splicing reaction. Catalysis depends on its core structure comprising two helical domains, P4–P6 and P3–P7. The two domains are joined by three sets of conserved base-triple(s) and other tertiary interactions. We found that the disruption of J8/7 X P4, one such conserved base-triple, causes the catalytic ability to deteriorate without altering the folding rate. This suggests that the base-triple stabilizes the active structure of the ribozyme but plays no significant role in RNA folding. By combining the present and previous results, it can be concluded that three sets of conserved base-triples play distinct roles in the *Tetrahymena* ribozyme.

Key words: group I intron, ribozyme, RNA-folding, self-splicing, *Tetrahymena*.

The *Tetrahymena* group I intron RNA is a large ribozyme composed of multiple structural domains (*1–4*). Its core region consists of two highly conserved domains, P4–P6 and P3–P7, recognizes two splice-sites, and conducts a self-splicing reaction (*1, 5*). These two domains are connected covalently by two single stranded regions, J3/4 and J6/7, that set the domains to form the active structure (N) (Fig. 1A) (*6–9*). Peripheral elements, located outside the core region, are connected *via* long-range interactions to form an "RNA cage," which stabilizes the active-3D structure of the core region (*1, 3, 10*).

Recent analyses revealed that multiple pathways exist for the folding of large ribozymes such as the *Tetrahymena* intron RNA and the RNaseP RNA (*11–14*). The folding proceeds in a hierarchical manner in the dominant pathway of the *Tetrahymena* ribozyme (Fig. 1B) (*15, 16*). In this pathway, a highly stable P4–P6 domain folds rapidly to form the intermediate (I_2), which is converted to another intermediate (I_3) by the formation of two sets of base-triples (J3/4 X P6 and J6/7 X P4) between J3/4, J6/7, and P6, P4, respectively. I_3 then conducts the folding of the P3–P7 domain to form I_F at a rate distinctively slower than that of P4–P6 formation. In the final step, a conformational rearrangement of the core region proceeds to establish the catalytically active structure (N) (*15–18*). Rearrangement of the core region has been suggested to occur in the "RNA cage" because the conversion from I_F to N is slower than the formation of the RNA cage (*17, 19*). In contrast, folding proceeds in a concerted manner in a minor pathway (*13, 14, 20, 21*). Each domain folds independently so that the ribozyme is assembled quite rapidly in this case and the pathway is observed as the initial burst in the kinetic folding analyses in minute-order time resolution (see zero time point of Figs. 3C and 4E) (*13, 19*).

The assemblage of the P4–P6 and the P3–P7 domains is assisted by the tertiary interactions of the phylogenetically conserved base-triples (*6, 7, 9*). J3/4 X P6 and J6/7 X P4 are involved in the consecutive base-triples constituting a triple-helical scaffold in the ribozyme 3D structure (*22*). J3/4 X P6 and J6/7 X P4, which align side by side in the crystal structure, assist in the assemblage of the two core domains. J6/7 X P4 mainly contributes to inducing P3–P7 folding, whereas J3/4 X P6 regulates the rearrangement from I_F to the active form in folding (*16, 23*). J6/7 has been shown to form base-triples by interacting with base moieties in the major groove of P4, and J3/4 has been proposed to form base-triples by interacting with a ribose-2′ OH in the minor groove of P6 (*7, 8*).

Another base-triple between the J8/7 region and the P4 stem (J8/7 X P4) is also phylogenetically well conserved: The sixth nucleotide of J8/7 (position 305) interacts with a major groove side of the fifth base-pair of the P4 stem (Fig. 1C) (*24, 25*). Mutational analyses of the self-splicing reaction showed that the disruption of this triple reduces ribozyme activity at low Mg^{2+} or high temperature, indicating that this triple also plays a crucial role in assembling the two core domains (*24, 25*). We investigated the role of this particular triple by employing derivatives of the *Tetrahymena* ribozyme.

MATERIALS AND METHODS

Preparation of RNAs—Plasmids encoding the mutant ribozymes employed in this study were prepared from the pTZIVSU plasmid (*26*) using polymerase chain reaction (PCR)–based, site-directed mutagenesis as described (*27*). The resulting constructs were verified by DNA sequencing. The template DNAs for *in vitro* transcription of L-21 *Sca*I forms of the *Tetrahymena* ribozyme and its mutants were generated by 20 cycles of PCR using KOD DNA polymerase (Toyobo, Tokyo). For PCR, 1 ng of a template plasmid (a derivative of pTZIVSU) and the following set of primers

[1] This work was supported by Grants-in-Aid for Scientific Research on Priority Areas (T. Inoue) and the Encouragement of Young Scientists (No. 13780554, Y. Ikawa) from the Ministry of Education, Science, Sports and Culture of Japan.

[2] To whom correspondence should be addressed. E-mail: tan@kuchem.kyoto-u.ac.jp

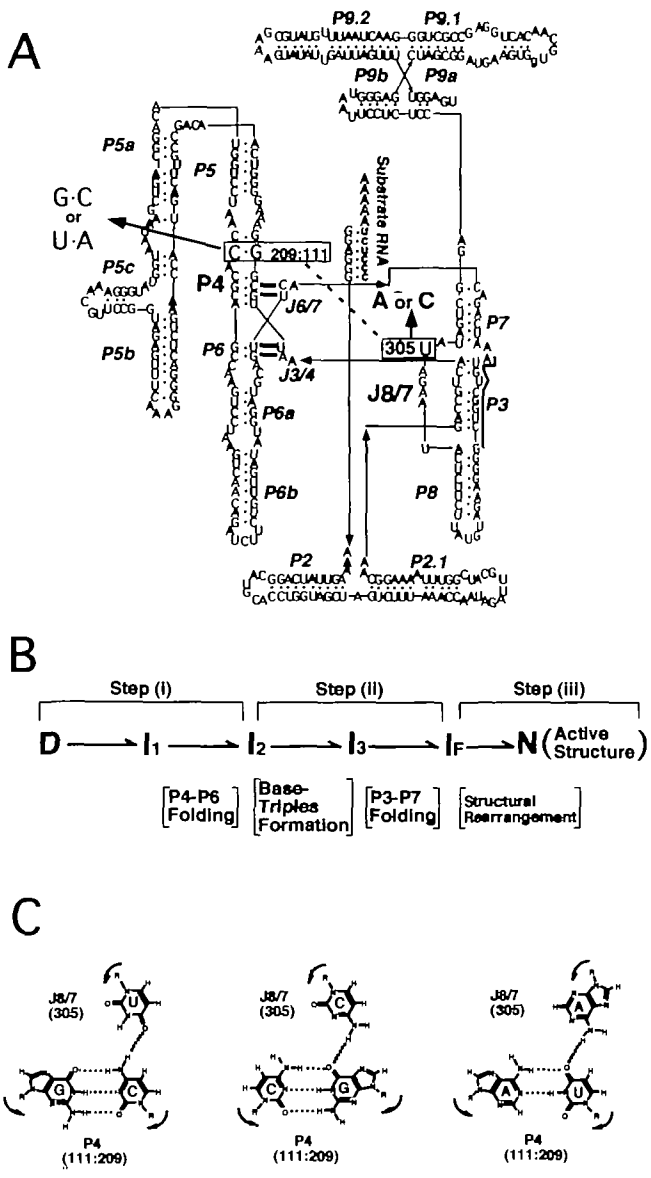

Fig. 1. **The structure and folding pathway of the *Tetrahymena* ribozyme.** A: Secondary structure of the L-21 *Tetrahymena* ribozyme (*3, 33*). Small arrowheads superimposed on lines indicate 5′-to-3′ polarity. The substrate RNA for the gain of activity assay is indicated by outline (*15*). The sequences targeted by oligonucleotide probes are indicated with bold lines (*15, 29*). A broken line indicates the conserved base-triple between the sixth nucleotide of the J8/7 region and the fifth base-pair of the P4 stem. Bold lines indicate J3/4 X P6 and J6/7 X P4 base-triples (*7, 8*). Positions with introduced base-substitutions (G111, C209, and U305) are boxed. Base-substitutions employed in this study are indicated by large arrows; U305C, U305A, G111C/C209G, or C209G/U305C (*24, 25*). B: A simplified scheme of the folding pathway of the core region of the L-21 *Tetrahymena* ribozyme. I_1 and I_2 represent the folding intermediates in which the P4–P6 domain forms secondary and tertiary structures, respectively (*16*). I_3 represents the intermediate in which the P4–P6 domain and four consecutive base-triples are formed. I_F represents the intermediate in which both the P4–P6 and P3–P7 domains are folded. The rate constant of steps (i), (ii), and (iii) can be determined experimentally by measuring the rate of P4–P6 domain folding, P3–P7 domain folding, or active structure formation, respectively. C: Model base-triples between J8/7 and P4 (*24, 25*). Arrows denote strand polarity. (Left) wild type (G111/C209/U305). (Middle) G111C/C209G/U305C mutant. (Right) G111A/C209U/U305A mutant.

were used: 5′-TAATACGACTCACTATAGGGCGTCAAAT-TGGGGGAAAGG-3′ (the promoter sequence for T7 RNA polymerase is underlined) and 5′-ACTCCAAAACTAAT-CAATAT-3′. *In vitro* transcription reactions with T7 RNA polymerase were performed as described (*28*).

Gain of Activity Assay—The gain of activity assay for measurement was performed as described (*15, 29*). The final concentration of L-21 *Sca*I ribozyme and the substrate RNA labeled at the 5′ terminus with ^{32}P (5′-CCCUCUA-AAAA-3′), were 20 and 16 nM, respectively. Cleavage reactions were performed for 30 s. Procedures for the gain of activity assay were identical at 2 and 1 mM Mg^{2+} except for the final concentration of magnesium ions in the folding buffer. The assays were repeated three times. The experimental errors represent the standard deviations of three independent experiments.

Kinetic Oligonucleotide Hybridization Assay—The kinetic oligonucleotide hybridization assay was performed as described (*15, 29, 30*). For the measurement of the folding kinetics of the P3–P7 domain, a uniformly ^{32}P-labeled L-21 *Sca*I ribozyme (1 nM) and oligonucleotide probes (20 nM) complementary to the P3 region (positions A270–G279) were used as described (*16, 19*). Procedures for the assay were identical at 2 and 1 mM Mg^{2+} except for the final concentration of magnesium ions in the folding buffer. The assays were repeated three times. The experimental errors represent the standard deviations of three independent experiments.

RESULTS AND DISCUSSION

Design of J8/7 X P4 Defective Mutants—We first investigated derivatives of the *Tetrahymena* ribozyme with mutations at the J8/7 X P4 base-triple. The J8/7 XP4 base-triple can be disrupted by either substituting the fifth base-pair in P4 (G111/C209) or the sixth nucleotide of the J8/7 region (U305) to design a G111C/C209G mutation at P4, and a U305C or U305A mutation at J8/7 (Fig. 1A) (*24, 25*). However, recent analyses predict that substitutions in the J8/7 region also alter the relative stability between the native P3 structure that is essential for catalysis and the mispaired P3 (alt-P3) structure that inactivates the ribozyme (Fig. 2) (*31*). Thus a U305C or U305A mutation could stabilize or destabilize the alt-P3 structure and slow or enhance ribozyme folding, respectively. [Note: the U305G mutation has been shown to maintain the isosteric base-triples (*24, 25*).]

The above possibility was tested by preliminary characterization of the rate of active structure formation ($k_{overall}$) by employing the gain of activity assay, a standard technique for determining the rate of active ribozyme formation (*13–15*). The $k_{overall}$ values of the wild type and mutants differed significantly as predicted (Fig. 3). At 2 mM Mg^{2+}, which is the optimal Mg^{2+} concentration for folding of the wild type ribozyme, the $k_{overall}$ of the U305C mutant (0.09 min^{-1}) was approximately one-tenth that of the wild type (0.95 min^{-1}), but close to that of a known slow-folding mutant C98A (0.07 min^{-1}), which contains a destabilized P3 (Figs. 2 and 3B) (*32*). The amount of substrate RNA cleaved at zero time in the case of U305A (the initial burst) was 8.0 nM. The initial burst represents the ribozyme molecules that fold *via* a fast-folding pathway and complete folding within the first 30 s (*19*). This value was 2.5-fold higher

than that of the wild type (3.2 nM) and close to that of a previously characterized, fast folding mutant, U273A, which contains a highly stable P3 (8.4 nM, Figs. 2 and 3C) (*14, 32*). G111C/C209G exhibited folding kinetics similar to those of the wild type (Fig. 3A). Because of these observations, the P4 X J8/7 interaction was investigated with the three mutants that showed slow (U305C), normal (wild type and G111/C209 mutant), or fast (U305A) rates of folding. To restore the J8/7 X P4 interaction isosterically in the U305C and U305A mutants, two extra derivatives were also designed by introducing a mutation in the corresponding fifth base-pair of P4: G111C/C209G and G111A/C209U for U305C and U305A, respectively (Fig. 1C) (*25*).

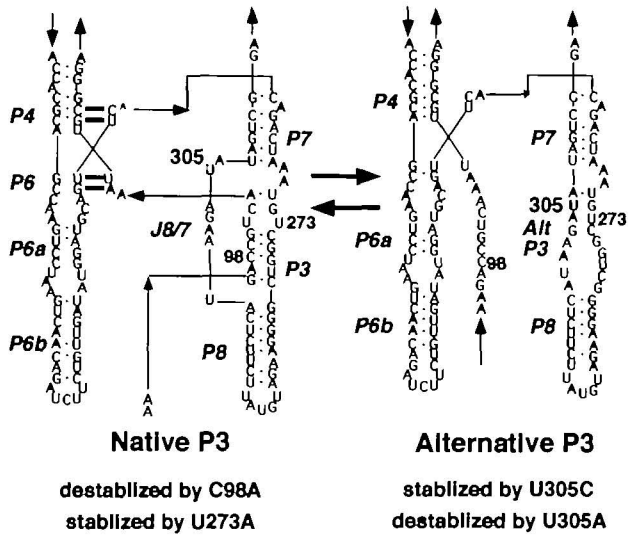

Fig. 2. **Alternative secondary structure of the catalytic core.** Alternative P3 pairings (right) possibly compete with the native P3 pairings (left) (*31*). Arrowheads superimposed on lines indicate 5′-to-3′ polarity. U305C or C98A base-substitutions stabilize the alternative P3 or destabilize the native P3, respectively. U305A or U273A base-substitutions destabilize the alternative P3 or stabilize the native P3, respectively.

Role of the J8/7 X P4 Base-Triple in the Ribozyme That Folds at a Normal Rate—The folding properties of the wild type and G111C/C209G ribozymes, which possess the same N- and alt-P3, were analyzed at either 1 or 2 mM Mg^{2+} where the wild type efficiently performs catalysis (Fig. 4A, Table I). The overall rates of active structure formation ($k_{overall}$) were determined by performing the gain of activity assay (*15, 29*). The rate of active structure formation of G111C/C209G (1.5 or 2.2 min^{-1} at 1 or 2 mM Mg^{2+}, respectively) was slightly larger than that of the wild type (0.95 or 1.7 min^{-1} at 1 or 2 mM Mg^{2+}, respectively), suggesting that the disruption of the base-triple slightly accelerates the rate of active structure formation for the ribozyme with a normal folding rate. However, the maximal efficacies for cleaving the substrate RNA (R_{max}) by G111C/C209G were less than those by the wild type after pre-folding at both 2 and 1 mM Mg^{2+} (Table II). R_{max} for the wild type ribozyme was almost the same at either 1 or 2 mM Mg^{2+} (Table II). However, R_{max} for G111C/C209G decreased from 10.9 to 7.2 nM/30 s when the Mg^{2+} concentration was reduced to 1 mM (Table II). These results suggest that the J8/7 X P4 base-triple contributes to maintaining the active structure, especially at 1 mM Mg^{2+}.

We also determined the folding properties of the P3–P7 domain by using the oligonucleotide hybridization assay (*15, 29*) to see whether the different catalytic abilities of the active structure at 1 mM Mg^{2+} can be attributed to the stabilities of their P3–P7. The equilibrium endpoint (f_{fin}) of oligonucleotide hybridization was determined because it serves as an index of the stability of the folded P3–P7 (*16, 19, 21*). At 1 mM Mg^{2+}, the f_{fin} values of P3–P7 formation of the two ribozymes were close (Table III), indicating that disruption of the base-triple does not influence the stability of P3–P7. In the hierarchical folding process of the *Tetrahymena* ribozyme, the stability of P3–P7 reflects the stability of an intermediate structure, I_P that possesses a folded P3–P7 (Fig. 1B). Thus, it is concluded that the J8/7 X P4 base-triple contributes to stabilizing the active ribozyme structure.

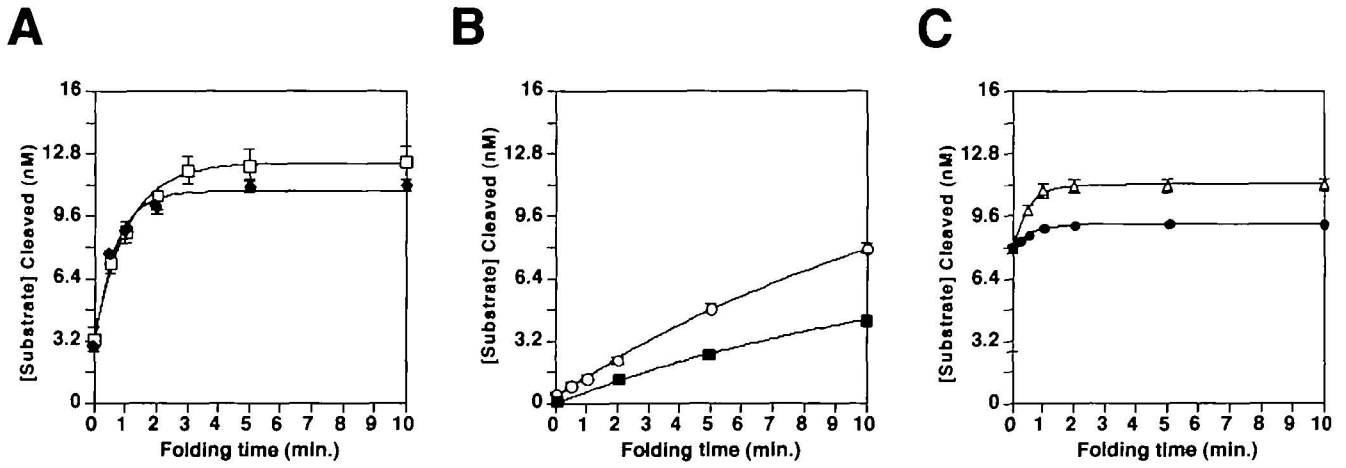

Fig. 3. **Folding kinetics of the wild type ribozyme and its slow and fast folding mutants.** A: Kinetics of active structure formation for the wild type ribozyme (open squares) and the G111C/C209G mutant (filled diamonds) at 2 mM Mg^{2+}. B: Kinetics of active structure formation for the slow folding mutants. U305C (open circles) and C98A (filled squares), at 2 mM Mg^{2+}. C: Kinetics of active structure formation for the fast folding mutants. U305A (open triangles) and U273A mutant (filled circles) at 2 mM Mg^{2+}.

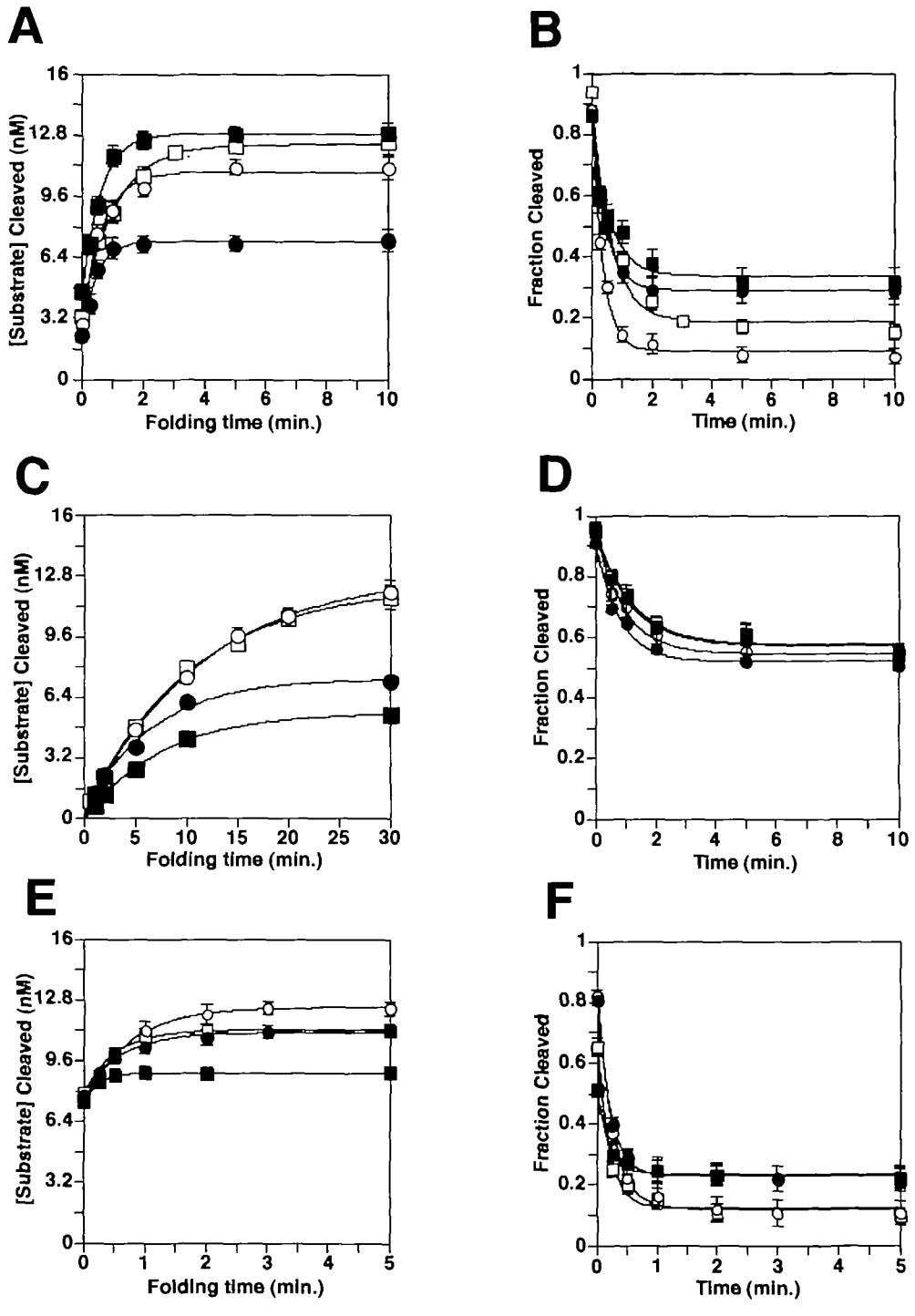

Fig. 4. **Effects of disruption of J8/7 X P4 base-triple.** Kinetics of active structure formation (A, C, E) or P3–P7 domain folding (B, D, F) of normal folding ribozymes (A, B), slow folding mutants (C, D) or fast folding mutants (E, F). A: Kinetics of active structure formation of the wild type ribozyme at 2 (open squares) or 1 mM Mg^{2+} (filled squares) and the G111C/C209G mutant at 2 (open circles) or 1 mM Mg^{2+} (filled circles). B: Kinetics of P3 helix formation of the wild type ribozyme at 2 (open squares) or 1 mM Mg^{2+} (filled squares) and the G111C/C209G mutant at 2 (open circles) or 1 mM Mg^{2+} (filled circles). C: Kinetics of active structure formation of the U305C mutant at 2 (open squares) or 1 mM Mg^{2+} (filled squares) and the G111C/C209G/U305C mutant at 2 (open circles) or 1 mM Mg^{2+} (filled circles). D: Kinetics of P3–P7 domain formation of the U305C mutant at 2 (open squares) or 1 mM Mg^{2+} (filled squares) and the G111C/C209G/U305C mutant at 2 (open circles) or 1 mM Mg^{2+} (filled circles). E: Kinetics of active structure formation of the U305A mutant at 2 (open squares) or 1 mM Mg^{2+} (filled squares) and the G111A/C209U/U305A mutant at 2 (open circles) or 1 mM Mg^{2+} (filled circles). F: Kinetics of P3–P7 domain formation of the U305A mutant at 2 (open squares) or 1 mM Mg^{2+} (filled squares) and the G111A/C209U/U305A mutant at 2 (open circles) or 1 mM Mg^{2+} (filled circles).

Role of the J8/7 X P4 Base-Triple in a Slow Folding Ribozyme—We next investigated the role of the J8/7 X P4 base-triple in the U305C mutant, which folds distinctly more slowly than the wild type. The mispaired form of P3 pairing (alt-P3) in this mutant is stabilized (Figs. 2 and 3B). As a control with an undisrupted J8/7 X P4 base-triple, we employed the G111C/C209G/U305C mutant, which has the same N- and alt-P3 sequences as the U305C mutant but possesses an alternative J8/7 X P4 base-triple (Fig. 1C, middle). At 2 mM Mg^{2+}, both the rates of active structure formation (Table I) and the maximal efficacies of the cleavage reaction (R_{max}) after pre-folding were quite comparable for both ribozymes (Table II). The thermodynamic stability of the folded P3–P7 (f_{fln} of the oligonucleotide hybridization assay) was also comparable for the two ribozymes, although their f_{fln} values were larger than that of the wild type, presumably because the P3 regions of the mutants are in equilibrium between the native and alternative-P3 structure (Table III).

At 1 mM Mg^{2+}, in contrast, the R_{max} of the G111C/C209G/U305C mutant (7.4 nM/30 s) was 1.3-fold greater than that of the U305C mutant (5.6 nM/30 s) after prefolding (Table

TABLE I. **The rate constants of active ribozyme formation ($k_{overall}$; min^{-1}) of the wild type and derivatives.**

	J8/7 X P4	2 mM Mg^{2+}	1 mM Mg^{2+}
(normal folding ribozyme)			
Wild type	+	0.95 ± 0.04	1.7 ± 0.1
G111C/C209G	–	1.5	2.2 ± 0.1
(slow folding ribozyme)			
G111C/C209G/U305C	+	0.08	0.15 ± 0.01
U305C	–	0.09	0.12 ± 0.01
(fast folding ribozyme)			
G111A/C209U/U305A	+	1.4 ± 0.2[a]	1.6 ± 0.1[a]
U305A	–	2.0 ± 0.1[a]	4.3 ± 0.3[a]

[a]The majority of the molecules folded *via* a fast-folding pathway (see the zero time points in Fig. 4E).

TABLE II. **The maximal efficiency of the reaction (R_{max}, nM/30 s) by the wild type and derivatives.**

	J8/7 X P4	2 mM Mg^{2+}	1 mM Mg^{2+}
(normal folding ribozyme)			
Wild type	+	12.3 ± 0.8	13.0 ± 0.8
G111C/C209G	–	10.9 ± 0.3	7.2 ± 0.1
(slow folding ribozyme)			
G111C/C209G/U305C	+	13.0 ± 0.6	7.4 ± 0.2
U305C	–	12.3 ± 0.1	5.6 ± 0.2
(fast folding ribozyme)			
G111A/C209U/U305A	+	12.5 ± 0.3	11.0 ± 0.3
U305A	–	11.2 ± 0.3	9.0 ± 0.3

II). A similar observation for R_{max} at low Mg^{2+} concentration has been reported for other slow folding mutants (*32*). However, it is unclear why the R_{max} of the G111C/C209G/U305C mutant at 1 mM Mg^{2+} is smaller than that of the wild type. On the other hand, the stability of the P3–P7 domain (f_{fin}, Table III) was still quite comparable for the two ribozymes. These results suggest that the restored J8/7 X P4 base-triple (G111C/C209G/U305C) improves the stability of the active structure of the U305C mutant (Table II), but has no effect on the stability of the P3–P7 domain (f_{fin}, Table III) at 1 mM Mg^{2+}.

Role of the J8/7 X P4 Base-Triple in the Fast Folding Ribozyme—The U305A mutant, which folds very rapidly due to its destabilized alt-P3 structure, was investigated as described above. In addition to this mutant, the G111U/C209A/U305A mutant, which shares the same N- and alt-P3 sequence with the U305A mutant but possesses an alternative J8/7 X P4 base-triple, was prepared as a control molecule by introducing an additional mutation (G111U/C209A) in its P4 region (Fig. 1C, right).

At 2 mM Mg^{2+}, the initial burst fraction of the active structure (see zero time points of Fig. 4E) and the thermodynamic stability (f_{fin} of the oligonucleotide hybridization assay) were quite comparable for the two ribozymes (Table III), while the maximal efficiency for the cleavage reaction (R_{max}, Table II) of the G111U/C209A/U305A mutant (12.5 nM/30 s) was slightly better than that of the U305A mutant (11.2 nM/ 30 s). At 1 mM Mg^{2+}, the R_{max} of G111U/C209A/U305A (11 nM/30 s) was still better than that of U305A (9.0 nM/30 s) (Table II), while no differences were observed for the initial burst fraction (zero time points in Fig. 4E) or the stability of P3–P7 (Table III). These bindings suggest that the restored base-triple improves the stability of the active structure of the U305A mutant but has no influence on either the fast folding fraction or the stability of the P3–P7 domain.

TABLE III. **The equilibrium end points (f_{fin}) of P3–P7 formation for the wild type and derivatives.**

	J8/7 X P4	2 mM Mg^{2+}	1 mM Mg^{2+}
(normal folding ribozyme)			
Wild type	+	0.18 ± 0.04	0.34 ± 0.05
G111C/C209G	–	0.09 ± 0.02	0.29 ± 0.05
(slow folding ribozyme)			
G111C/C209G/U305C	+	0.54 ± 0.04	0.52 ± 0.01
U305C	–	0.58 ± 0.02	0.57 ± 0.03
(fast folding ribozyme)			
G111A/C209U/U305A	+	0.12 ± 0.05	0.23 ± 0.01
U305A	–	0.11 ± 0.03	0.24 ± 0.04

CONCLUSION

In the present study, the effects of the conserved base-triple between J8/7 and P4 on the folding rates and the stability of the active structure of the *Tetrahymena* ribozyme were investigated by employing the wild type ribozyme, and slow and fast folding mutants. For the wild type, the disruption of the base-triple resulted in a slight improvement in the rate of active structure formation ($k_{overall}$). However, it had no effect on the rate of active structure formation or on the fast folding fraction of the mutants, indicating that the base-triple plays no (or only a very minor) role in the kinetic folding of the wild type and mutant ribozymes. The J8/7 X P4 base-triple, however, improved the thermodynamic stability of the active ribozyme structure. At 1 mM Mg^{2+}, the disruption of the base-triple caused the destabilization of the active structures of the wild type, slow and fast folding mutants. The base-triple–dependent stabilization is specific to the active ribozyme structure because the stability of the P3–P7 domain (or the intermediate I_F) was inert to disruption.

By combining the present analysis with the previous ones on the other base-triples, it can be concluded that the three sets of conserved base-triples in the core region of the *Tetrahymena* group I ribozyme play distinctly different roles in the ribozyme folding process (Fig. 1B). J3/4 X P6 improves the rate limiting rearrangement from I_F to N (*23*), J6/7 X P4 improves both the rate of I_F formation and stability of I_F (*16, 23*), while J8/7 X P4 improves the stability of N but not I_F.

We thank the members of the Inoue Laboratory for critical reading of the manuscript.

REFERENCES

1. Murphy, F.L. and Cech, T.R. (1993) An independently folding domain of RNA tertiary structure within the *Tetrahymena* ribozyme. *Biochemistry* **32**, 5291–5300
2. Jaeger, L., Michel, F., and Westhof, E. (1996) The structure of group I ribozymes in *Catalytic RNA* (Eckstein, F. and Lilley, D.M., eds.) pp. 33–52, Springer, Berlin
3. Lehnert, V., Jaeger, L., Michel, F., and Westhof, E. (1996) New loop-loop interactions in self-splicing introns of subgroup IC and ID. *Chem. Biol.* **3**, 993–1009
4. Ikawa, Y., Yoshioka, W., Ohki, Y., Shiraishi, H., and Inoue, T. (2001) Self-splicing of the *Tetrahymena* group I ribozyme without conserved base-triples. *Genes Cells* **6**, 411–420
5. Ikawa, Y., Shiraishi, H., and Inoue, T. (2000) Minimal catalytic domain of a group I self-splicing intron RNA. *Nat. Struct. Biol.* **7**, 1032–1035
6. Michel, F. and Westhof, E. (1990) Modelling of the three-demensional architecture of group I catalytic introns based on com-

parative sequence analysis. *J. Mol. Biol.* **216**, 585–610
7. Michel, F., Ellington, A.D., Couture, S., and Szostak, J.W. (1990) Phylogenetic and genetic evidence for base-triples in the catalytic domain of group I introns. *Nature* **347**, 578–580
8. Chastain, M. and Tinoco-Jr, I. (1992) A base-triple structural domain in RNA. *Biochemistry* **31**, 12733–12741
9. Green, R. and Szostak, J.W. (1994) *In vitro* genetic analysis of the hinge region between helical elements P5-P4-P6 and P7-P3-P8 in the sunY group I self-splicing intron. *J. Mol. Biol.* **235**, 140–155
10. Ikawa, Y., Ohta, H., Shiraishi, H., and Inoue, T. (1997) Long-range interactions between the P2.1 and P9.1 domains of the *Tetrahymena* ribozyme. *Nucleic Acids Res.* **25**, 1761–1765
11. Pan, J., Thirumalai, D., and Woodson, S.A. (1997) Folding of RNA involves parallel pathways. *J. Mol. Biol.* **273**, 7–13
12. Pan, T., Fang, X., and Sosnick, T. (1999) Pathway modulation, circular permutation and rapid RNA folding under kinetic control. *J. Mol. Biol.* **286**, 721–731
13. Russell, R. and Herschlag, D. (1999) New pathways in folding of the *Tetrahymena* group I RNA enzyme. *J. Mol. Biol.* **291**, 1155–1167
14. Pan, J., Deras, M.L., and Woodson, S.A. (2000) Fast folding of a ribozyme by stabilizing core interactions: evidence for multiple folding pathways in RNA. *J. Mol. Biol.* **296**, 133–144
15. Zarrinkar, P.P. and Williamson, J.R. (1994) Kinetic intermediates in RNA folding. *Science* **265**, 918–924
16. Zarrinkar, P.P. and Williamson, J.R. (1996) The kinetic folding pathway of the *Tetrahymena* ribozyme reveals possible similarities between RNA and protein folding. *Nat. Struct. Biol.* **3**, 432–438
17. Sclavi, B., Sullivan, M., Chance, M.R., Brenowitz, M., and Woodson, S.A. (1998) RNA folding at millisecond intervals by synchrotron hydroxyl radical footprinting. *Science* **279**, 1940–1943
18. Chaulk, S.G. and MacMillan, A.M. (2000) Characterization of the *Tetrahymena* ribozyme folding pathway using the kinetic footprinting reagent peroxynitrous acid. *Biochemistry* **39**, 2–8
19. Rook, M.S., Treiber, D.K., and Williamson, J.R. (1999) An optimal Mg^{2+} concentration for kinetic folding of the *Tetrahymena* ribozyme. *Proc. Natl. Acad. Sci. USA* **96**, 12471–12476
20. Zhuang, X., Bartley, L.E., Babcock, H.P., Russell, R., Herschlag, D., and Chu, S. (2000) A single-molecule study of RNA catalysis and folding. *Science* **288**, 2048–2051
21. Treiber, D.K. and Williamson, J.R. (2001) Concerted kinetic folding of a multidomain ribozyme with a disrupted loop-receptor interaction. *J. Mol. Biol.* **305**, 11–21
22. Cate, J.H., Gooding, A.R., Podell, E., Zhou, K., Golden, B.L., Kundrot, C.E., Cech, T.R., and Doudna, J.A. (1996) Crystal structure of a group I ribozyme domain: Principles of RNA packing. *Science* **273**, 1678–1685
23. Ohki, Y., Ikawa, Y., Shiraishi, H., and Inoue, T. (2001) A deteriorated triple-helical scaffold accelerates formation of the *Tetrahymena* ribozyme active structure. *FEBS Lett.* **493**, 95–100
24. Tanner, M.A. and Cech, T.R. (1997) Joining the two domains of a group I ribozyme to form the catalytic core. *Science* **275**, 847–849
25. Tanner, M.A., Anderson, E.M., Gutell, R.R., and Cech, T.R. (1997) Mutagenesis and comparative sequence analysis of a base triple joining the two domains of group I ribozymes. *RNA* **3**, 1037–1051
26. Williamson, C.L., Desai, N.M., and Burke, J.M. (1989) Compensatory mutations demonstrate that P8 and P6 are RNA secondary structure elements important for processing of a group I intron. *Nucleic Acids Res.* **17**, 675–689
27. Imai, Y., Matsushima, Y., Sugimura, T., and Terada, M. (1991) A simple and rapid method for generating a deletion by PCR. *Nucleic Acids Res.* **19**, 2785
28. Milligan, J.F., Groebe, D.R., Witherell, G.W., and Uhlenbeck, O.C. (1987) Oligoribonucleotide synthesis using T7 RNA polymerase and synthetic DNA templates. *Nucleic Acids Res.* **15**, 8783–8798
29. Zarrinkar, P.P. and Williamson, J.R. (1996) The P9.1–P9.2 peripheral extension helps guide folding of the *Tetrahymena* ribozyme. *Nucleic Acids Res.* **24**, 854–858
30. Treiber, D.K. and Williamson, J.R. (2000) Kinetic oligonucleotide hybridization for monitoring kinetic folding of large RNAs in *Methods in Enzymology* (Celander, D.W. and Abelson, J.N., eds.) Vol. 317, pp. 330–353, Academic Press, New York
31. Pan, J. and Woodson, S.A. (1998) Folding intermediates of a self-splicing RNA: mispairing of the catalytic core. *J. Mol. Biol.* **280**, 597–609
32. Ohki, Y., Ikawa, Y., Shiraishi, H., and Inoue, T. (2002) Mispaired P3 region in the hierarchical folding pathway of the *Tetrahymena* ribozyme. *Genes Cells* **7**, 851–860
33. Cech, T.R., Damberger, S.H., and Gutell, R.H. (1994) Representation of the secondary and tertiary structure of group I introns. *Nat. Struct. Biol.* **1**, 273–280